

A tunable bidirectional SH waves transducer based on antiparallel thickness-shear (d_{15}) piezoelectric strips

Mingtong Chen^{1,2}, Qiang Huan^{1,2}, Zhongqing Su³, Faxin Li^{1,2,a)}

¹ LTCS and College of Engineering, Peking University, Beijing 100871, China

² Center for Applied Physics and Technology, Peking University, Beijing, China

³ Department of Mechanical Engineering, The Hong Kong Polytechnic University, Hung Hom, Kowloon, Hong Kong SAR, P.R. China

Abstract

Guided wave based defects inspection is very promising in the field of structural health monitoring (SHM) and nondestructive testing (NDT) due to its less dissipation and thus long distance coverage. In comparison with the widely used Lamb waves, shear horizontal (SH) waves are relatively simple but less investigated probably due to the traditional notion that SH waves were usually excited by electromagnetic acoustic transducers (EMAT). In this work, we proposed a tunable method to excite single-mode bidirectional SH waves in plates using antiparallel thickness-shear (d_{15}) piezoelectric strips (APS). The proposed SH wave driving mechanism here is similar to that by using the periodic permanent magnetics (PPM) based EMAT with the period of strips equal to half of the wavelength. Both finite element simulations and experiments were conducted to validate this transducer in excitation of bidirectional SH waves. Results show that the Lamb waves excited by single piezoelectric strip can be suppressed very well. The radiation angle of the excited bidirectional SH wave can be reduced by extending the strip length, increasing the driving frequency or using more strips. Moreover, the APS transducer can selectively excite SH_1 wave and suppress the SH_0 wave at 174kHz and 273kHz in a 10mm-thick aluminum plate. Considering its simple structure, flexible design and low excitation energy, the APS

^{a)} Author to whom all correspondence should be addressed, Email: lifaxin@pku.edu.cn

SH wave transducer is expected to be widely used in near future.

Keywords: Guided wave; Shear horizontal wave; piezoelectric transducer; thickness-shear; electromagnetic acoustic transducer (EMAT)

1. Introduction

Ultrasonic guided wave had been more and more widely used in the field of nondestructive testing (NDT) and structural health monitoring (SHM) due to its less dissipation and thus long distance (large area) coverage [1-4]. In plate-like structures, both Lamb waves and shear horizontal (SH) waves can exist. SH waves only have one displacement component which is parallel to the plate surface and perpendicular to the wave propagation direction [5]. Theoretically, the wave modes of SH waves are much simpler than that of the Lamb waves. However, in practice, SH waves were less used than Lamb waves, probably due to the traditional notion that SH waves were usually excited by electromagnetic acoustic transducers (EMAT) which required high energy in excitation and signal amplification circuit in reception.

In late 1970s, Thompson and co-workers proposed two type of EMATs to excite SH waves in plates: one is composed of periodic permanent magnetics (PPM) based on the Lorentz force which applied for non-ferromagnetic metallic plates [6]; the other is based on in-plane magnetostriction which can only be used for ferromagnetic materials [7]. Kwun et al excited longitudinal, torsional and flexural wave modes in rods and pipes using magnetostrictive EMAT [8] and magnetostrictive patch transducers (MPT) [9], respectively, and found the latter is superior to the former. Kim et al proposed different configurations of MPTs for pipes and plates [10,11] and they also designed omni-directional SH wave MPTs for plate structures [12,13]. Ribichini et al comparatively investigated the above-mentioned three types of EMATs in SH wave excitation/reception and concluded that both the PPM EMAT and MPT are superior to the magnetostrictive EMAT for steel plates [14]. Furthermore, the energy transfer efficiency the MPT is about one order higher than the PPM EMAT.

Based on the PPM EMAT and MPT, some fundamental characteristics of SH waves had been experimentally studied [15,16] and SH wave based defect inspection in plates were conducted [17-19].

Actually, SH waves can also be excited by piezoelectrics. It is well known that a thickness-shear (d_{15}) piezoelectric transducer can excite SH waves perpendicular to its poling direction but simultaneously excite Lamb waves along the poling direction [20]. Recently, Boivin et al show that the Lamb waves can be well suppressed (-16dB) at high drive frequency if the d_{15} piezoelectric strip is very long [21]. Miao et al proposed that single-mode SH wave can be excited/received by face-shear (d_{24}) piezoelectric transducers [22] or the synthetic face-shear mode piezoelectric wafers [23]. Bi-directional SH waves can also be excited, using dual face-shear (d_{24}) piezoelectric wafers [24]. Omni-directional SH wave piezoelectric transducers were also developed, based on the synthetic circumferential poling using d_{15} and d_{24} piezoelectric wafers [25,26], or based on thickness-poled, thickness-shear piezoelectric rings [27,28]. Based on d_{15} piezoelectric SH wave transducers, the interactions of SH wave with cracks were systematically investigated [29,30]. Thickness gauging of plate [31], defect inspection in bending plate [32] and composites [33], structural health monitoring of plates using sparse array [34] and phased array [35], were also conducted based different SH wave piezoelectric transducers. Recently, Li et al established a fully-coupled dynamic model for SH_0 wave excitation in plates using d_{15} piezoelectric strips [36], which had been validated by both finite element simulations and experiments at tuning frequencies.

It should be noted that the conventional EMATs based on PPM or magnetostrictively coupled meander-coil are by default bi-directional SH wave transducers, which can focus the wave energy in a controlled radiation angle and thus very promising in excitation of circumferential SH waves in pipes [37,38], or studying the fundamental characteristics of SH waves [15,16]. Furthermore, the EMAT based SH wave transducers usually can selectively excite single-mode SH waves in large

frequency-thickness-product plates [15,16,18], e.g., suppressing SH_0 wave and exciting single-mode SH_1 for tomography [18]. However, none of the above-mentioned piezoelectric SH wave transducers has the mode selective capacity.

In this work, we proposed that single-mode bi-directional SH waves can be excited by antiparallel shearing line forces and the line forces can be provided either by PPM EMAT or d_{15} mode piezoelectric strips. Thus, a novel bi-directional SH wave transducer based on antiparallel d_{15} piezoelectric strips (APS) is proposed. Firstly, the working principle of this bidirectional SH wave transducer is presented at Section 2. Then, in Section 3, finite element simulations were employed to predict the performances of the APS based SH wave transducers with different strip lengths, spacing and strip numbers. Later, experiments were conducted to examine the performances of the proposed transducer in Section 4. Discussions were presented in Section 5 and conclusions were summarized in Section 6. The proposed bi-directional piezoelectric SH wave transducer can be widely used in NDT/SHM and specially suitable for studying the fundamental properties of SH waves, such as reflection, refraction, mode conversion, etc.

2. Methods

2.1 Working Principle

As shown in Fig.1(a), an alternating shearing line force (with the frequency f) along the x_2 axis will excite largest SH waves in the x_1 direction and largest Lamb waves in the x_2 direction [5,39]. The radiation angle (2θ) of the excited SH waves and Lamb waves depend on the length (L) of the line force and the driving frequency, which can reach π for the point force case [40]. In the case of a pair of antiparallel alternating shearing force with the interval of T , as shown in Fig.1(b), the Lamb waves in the lateral far field (x_2 direction) will diminish via destructive interference. Meanwhile, the SH wave in the x_1 direction with the wavelength (λ) of $2T$ will be strengthened via constructive interference. Thus bidirectional SH wave is expected to be excited by such a pair of alternating, antiparallel shearing line force. Actually, this is the principle

of SH wave excitation using PPM EMAT in which the Lorentz force serves as the shearing line force [6]. Here we proposed that the alternating shearing line force can also be provided by using thickness-shear (d_{15}) piezoelectric strips conveniently driven by electric field. Furthermore, as the energy conversion efficiency of piezoelectric transducers is much higher than that of EMAT, one pair of antiparallel d_{15} piezoelectric strips (APS) should be capable of exciting SH wave with enough amplitude. That is, the structure of the APS SH wave transducer would be much simpler than the PPM EMAT where several pairs of permanent magnetics are required to enhance the excitation energy.

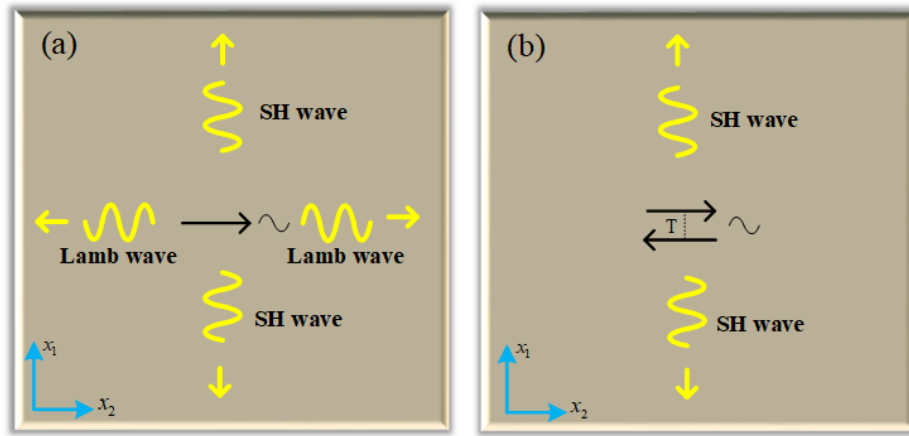


Fig.1 The guided wave modes in a large plate generated by: (a) single shearing line force; (b) antiparallel shearing line force.

The principle of SH wave mode selection of the APS transducer is similar to that of PPM EMAT. When the wavelength of SH_1 mode equals double wavelength of the SH_0 mode, and the strip interval equals the SH_0 wavelength, i.e., $\lambda_{SH1} = 2\lambda_{SH0}$, and $T = \frac{\lambda_{SH1}}{2} = \lambda_{SH0}$, the SH_0 mode will diminish via destructive interference and the SH_1 mode will be strengthened via constructive interference. The frequency-thickness product (fd) for this condition can be directly calculated from the following explicit phase velocity of SH waves:

$$c_p(fd) = \pm 2c_T \left\{ \frac{fd}{\sqrt{4(fd)^2 - n^2c_T^2}} \right\} \quad (1)$$

Where c_T is the velocity of bulk shear wave, n is the order of the SH mode.

Actually, as long as $T = n\lambda_{SH0} \neq m\lambda_{SH1}$ (where both n and m are integers), the SH₀ mode will diminish and only SH₁ mode will be excited.

Theoretically, when $T = \lambda_{SH1} = 1.5\lambda_{SH0}$, the SH₁ mode will diminish and SH₀ mode will be strengthened. However, in practice, it is rather difficult to suppress the dispersive SH₁ mode and excite single-mode SH₀ wave in large fd waveguide. Thus, single-mode SH₀ wave was usually excited below the cut-off frequency of the SH₁ wave.

2.2 Finite element simulations

To analyze the wave radiation patterns and the bidirectivity of the APS transducers, a three-dimensional finite element model was constructed using the ANSYS software. The material parameters of the PZT-5H strips used in the simulations were listed in Table I. An aluminum plate with the dimension of 400×400×1mm³ is used as waveguide and its density, Young's modulus, Poisson ratio are 2700 kg/m³, 71GPa and 0.33, respectively. The piezoelectric strips were modeled by SOLID 5 elements and the plate was modeled by SOLID 185 elements in the ANSYS software. The APS transducer bonded at the center of the plate is driven by 20V voltage signal (five-cycle Hanning windows-modulated sinusoid tone burst) and the radial displacement component u_r , tangential displacement component u_θ , and out-of-plane displacements component u_z were extracted at the distance (100mm) from the center of the APS. The largest size of elements was set to be less than 1/15 of the shortest wavelength and the time step was set to be less than 1/20 of the central frequency of the drive signal.

2.3 Experimental

Experiments were performed to explore the bidirectivity and the mode selection

capacity of the proposed APS transducer, respectively. The experimental setup was shown in Fig.2. For the bidirectivity testing, a thin aluminum plate with dimensions of $1000 \times 1000 \times 1 \text{ mm}^3$ was employed as the waveguide and the APS transducer was bonded on the plate using 502 epoxy adhesive with the bonding layer thickness of less than $20 \mu\text{m}$. The d_{15} piezoelectric strips were fabricated by commercial PZT-5H piezoelectric ceramics (Baoding Hongsheng Ceramic Inc., Hebei, China) with different dimensions and the material properties were listed in Table I. Two kinds of receivers were used in the experiment, one is the d_{15} type sensor with the dimensions of $12 \times 2 \times 0.8 \text{ mm}^3$ for receiving SH wave, the other is the d_{31} type sensor with the dimensions of $6 \times 6 \times 1 \text{ mm}^3$ for receiving Lamb waves. The d_{15} type sensor were bonded at the distance of 650mm from the excitation source and the d_{31} type sensor were bonded at the distance of 360mm. For the mode selective SH wave excitation, a thick aluminum plate with dimensions of $1200 \times 400 \times 10 \text{ mm}^3$ was used to generate higher mode SH waves at relatively low frequency. The d_{15} type sensors were also used in this experiment and it was 400mm away from the excitation source. All the actuators were driven by five-cycle sinusoid tone-burst modulated into the Hanning window signal through a function generator (33220A, Agilent, USA). The driven signal was amplified by a power amplifier (7602M, KROHN-HITE, USA) and the received signals were measured and collected by an oscilloscope (DSO-X 3024T, Agilent, USA).

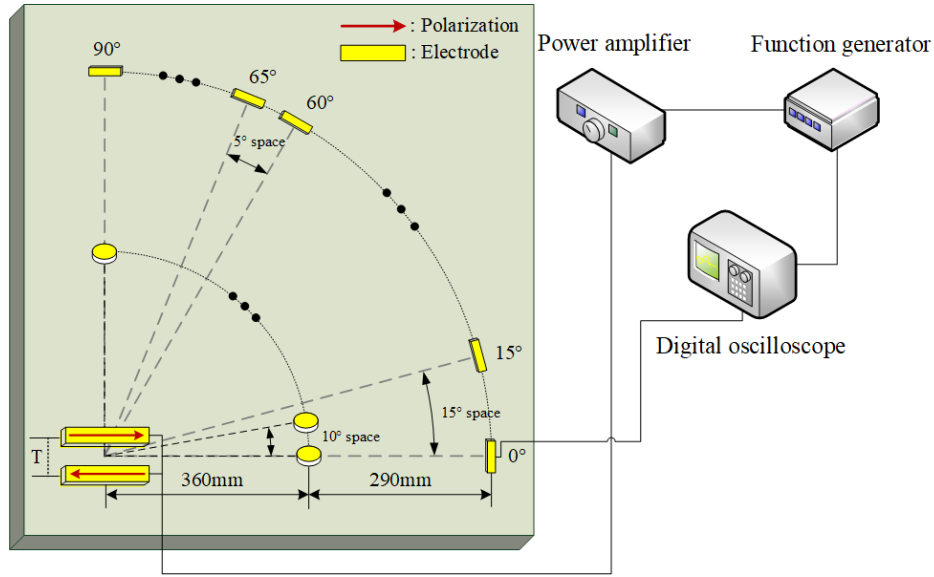


Fig2. Tesing setup for examining the performances of the proposed bidirectional SH wave transducer

Table I Material properties of the PZT-5H piezoelectric strip used in the simulations

Density ($\text{kg} \cdot \text{m}^{-3}$)	Relative dielectric constant		Piezoelectric constant ($\text{pC} \cdot \text{N}^{-1}$)		
ρ	$\epsilon_{33}^X / \epsilon_0$	$\epsilon_{11}^X / \epsilon_0$	d_{33}	$d_{31} = d_{32}$	$d_{15} = d_{24}$
7500	3400	3130	593	-274	741
Elastic compliances ($\text{pm}^2 \cdot \text{N}^{-1}$)					
$s_{11} = s_{22}$	s_{33}	s_{12}	$s_{13} = s_{23}$	$s_{44} = s_{55}$	s_{66}
16.5	20.7	-4.78	-8.45	43.5	42.6

3. Simulation results

We conducted a series of finite element simulations to examine the validity of the proposed bidirectional SH wave transducer based on antiparallel d_{15} piezoelectric strips (APS). Firstly, in Section 3.1 and 3.2, guided wave excitation by using

single/antiparallel shearing line forces and d_{15} piezoelectric strips were simulated, to check their differences in SH wave excitation. Then, in Section 3.3 and 3.4, the effects of strip interval (or driving frequency) and strip numbers on suppressing the Lamb waves, grating lobes of SH wave and reducing the radiation angles, were systematically investigated. Due to the computational complexity using the ANSYS software, high frequency simulations were not conducted nor the mode selectivity of the proposed APS SH wave transducers. In Section 3.5, the performances of multiple piezoelectric strips in one row were also simulated in generating bidirectional SH waves. Finally, in Section 3.6, a simplified theoretical model were employed to predict the radiation pattern of the excited SH_0 wave and comparison were made between theoretical results and simulation results.

3.1 Guided wave excitations by using single and antiparallel shearing line forces

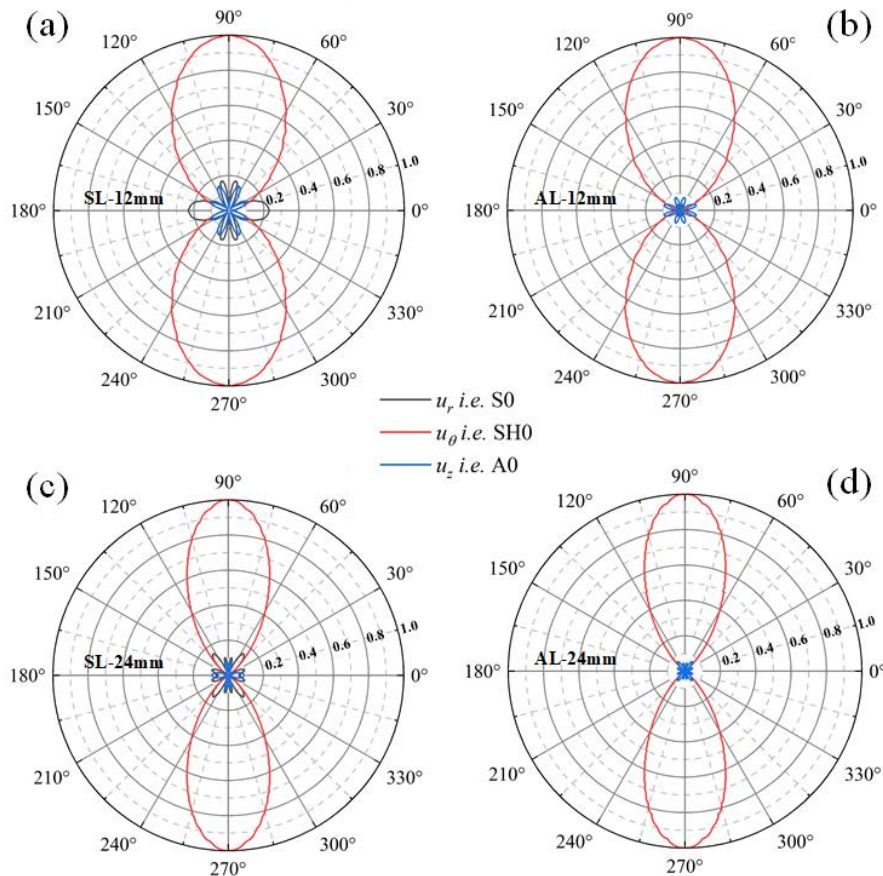


FIG3. Finite element simulated displacements of different guided wave modes generated in a 1mm-thick aluminum plate at 196kHz by using shearing line forces. Left: Single line force of (a) 12mm length (SL-12mm) and (c) 24mm length (SL-24mm); Right: Antiparallel line forces of (b) 12mm length (AL-12mm) and (d) 24mm length (AL-24mm). Interval between antiparallel line forces is 8mm.

Fig.3 shows the simulated displacements of different guided wave modes generated in a 1mm-thick aluminum plate at 196kHz using shearing line forces which was realized by??? in the FEM simulation . In Fig.3, the circumferential displacement u_θ denotes the SH₀ wave, the radial displacement u_r denotes the S₀ wave and the out-of-plane displacement u_z denotes the A₀ wave. It can be seen from Fig.3(a) that a single shearing line force can excite SH₀ wave with the maximum amplitudes along 90° and 270° direction, and simultaneously excited Lamb waves (S₀ and A₀) with the maximum amplitudes along 0° and 180° direction. The ratio of the maximum u_L (u_r or u_z , whichever is larger) to maximum u_θ , or abbreviated as LSR, is about 24% for the single line force of 12mm length, and the half radiation angle θ of the excited SH₀ wave is about 65°. When two 12mm-long antiparallel shearing line forces were employed, the LSR reduced to be within 10%, as seen in Fig.3(b), which indicates that the antiparallel shearing line force is very effective in suppressing the Lamb waves. However, the radiation angle of the excited SH wave by the antiparallel line forces is just slightly smaller than that by single line force, indicating that the wave energy focusing function of the antiparallel line force is not significant.

When the length of the single line force increases to 24mm, the LSR decreased to be about 16% and the half radiation angle θ decreases to be about 45°, as seen in Fig.3(c). This indicates that increasing the length of the line force can also suppress the Lamb waves, but it is not as effective as the antiparallel line forces. Note that increasing the force length is very effective to focus the SH wave energy. In the case of antiparallel line forces of 24mm length, the excited SLR further decreases to be about 6%, as seen in Fig.3(d). As expected, the SH wave radiation angle almost keeps almost unchanged

compared to that in Fig.3(c).

3.2 Guided wave excitations by using single and antiparallel d_{15} piezoelectric strips

We further conducted the FEM simulations using the d_{15} piezoelectric strips of the same length as the line forces in Fig.3, and the results were shown in Fig.4. Note that in all the cases, the strip width is 2mm and the thickness is 0.8mm. The piezoelectric materials used here is PZT-5H and its properties is listed in Table I.

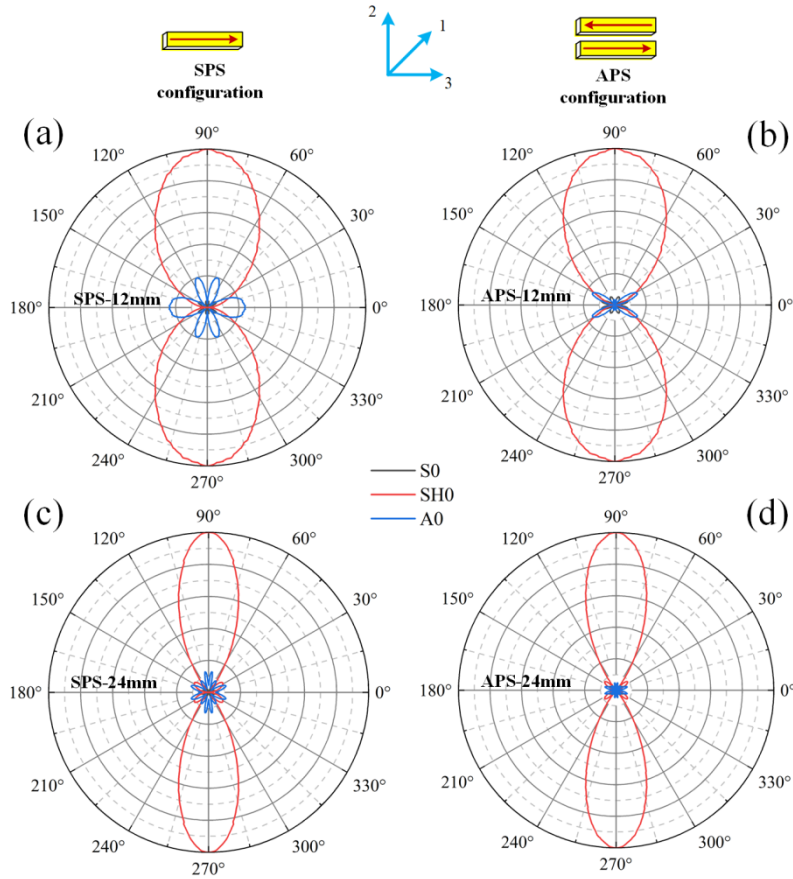


FIG4. Finite element simulated displacements of different guided wave modes generated in a 1mm-thick aluminum plate at 196kHz by using d_{15} piezoelectric strips with the width of 2mm and thickness of 0.8mm. Left: Single piezoelectric strip of (a) 12mm length (SPS-12mm) and (c) 24mm length (SPS-24mm); Right: Antiparallel piezoelectric strips of (b) 12mm length (APS-12mm) and (d) 24mm length (APS-24mm). Interval between antiparallel piezoelectric strips is 8mm.

It can be seen from Fig.4 that compared to the wave patterns generated by the shearing line forces in Fig.3, the wave patterns generated by the 2mm-wide, 0.8mm-thick d_{15} piezoelectric strips are similar. The excited LSR for the single piezoelectric strip case is very close to that for the single line force case, which is about 24% for the 12mm-long strip and 16-17% for the 24mm-long strip, as seen in Figs.4(a) and 3(c). However, for the antiparallel piezoelectric strips cases in Figs.4(b) and 4(d), the excited LSR is about 17% for the 12mm length case and about 10% for the 24mm length case, which are both larger than that of 10% and 6% by using the antiparallel line forces in Figs.3(b) and 3(d). This may be due to the finite thickness and finite width of the piezoelectric strips, compared to the zero-thickness, zero-width line force. To examine the effect of strip thickness and strip width on suppressing the Lamb waves, we further conducted FEM simulations using piezoelectric strips of different thickness (constant width of 2mm) and different widths (constant thickness of 0.8mm), and the results were shown in Fig.5.

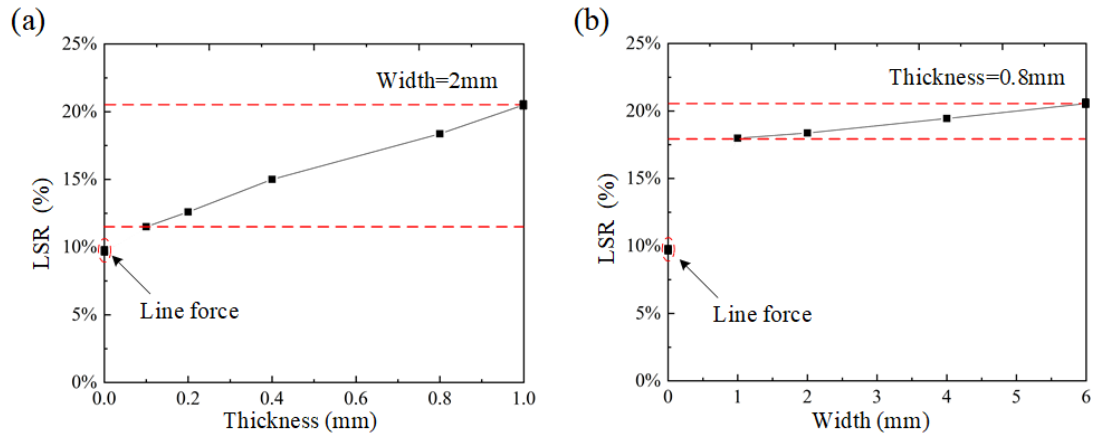


Fig.5 Effect of strip thickness and width on the excited LSR (ratio of maximum Lamb wave displacement to maximum SH wave displacement) using antiparallel d_{15} piezoelectric strips with the interval of 8mm (working frequency 196kHz). (a) constant width of 2mm; (b) constant thickness of 0.8mm.

It can be seen from Fig.5(a) that at the constant width of 2mm, the excited LSR using the APS increased steadily with the increasing thickness. However, at the constant

thickness of 0.8mm, the excited LSR just increased slightly with the increasing strip width, as seen in Fig.5(b). Therefore, the main differences of the excited LSR by using line forces and APS are due to the finite thickness of the APS. For a thicker strip, larger bending moment will be applied to the aluminum plate. In some directions, the bending moment induced by APS may be strengthened, leading to large grating lobes of the A_0 waves, as shown in Fig.4(b).

3.3 Effect of strip interval (or driving frequency) of the APS

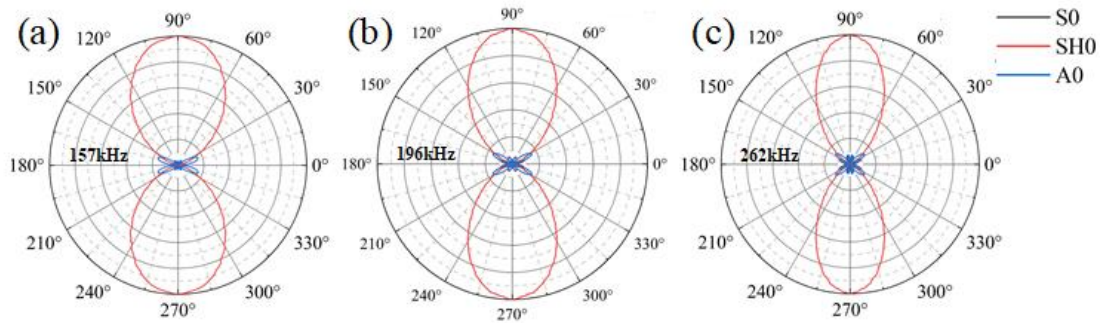


FIG.6 FEM simulated guided wave patterns excited by using antiparallel 12mm-long piezoelectric strips with different intervals (different exciting frequencies). (a) 10mm, 157kHz; (b)8mm, 196kHz; (c) 6mm, 262kHz.

Fig.6 shows the excited wave patterns by using one pair of 12mm-long APS at different strip intervals of 10mm, 8mm and 6mm, corresponding to driving frequencies of 157kHz, 196kHz and 262kHz, respectively. It can be seen that with the increasing driving frequency, the excited LSR decreased steadily from 16.5% (157kHz) to 13.6% (262kHz), and the half radiation angle of the excited SH wave also decreased steadily, from about 65° to 55° . This indicates that increasing driving frequency (decreasing the strip interval) is quite effective in suppressing the Lamb waves and focusing the SH wave energy.

3.4 Performances of multiple pairs of antiparallel piezoelectric strips

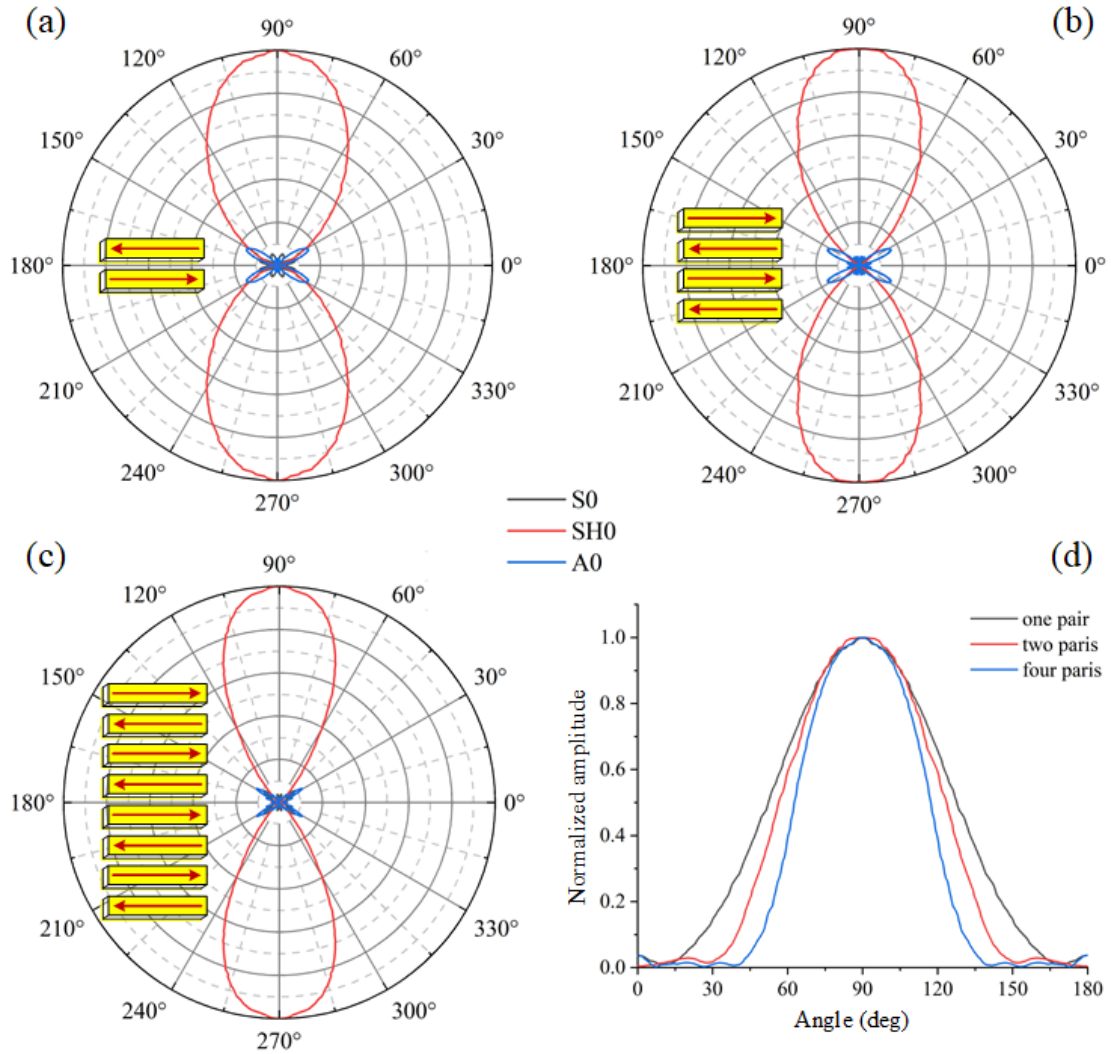


FIG.7 FEM simulated wave patterns excited by using several pairs of 12mm-long APS in one column. (a) one pair; (b) two pairs; (c) four pairs. (d) radiation angles of excited SH₀ wave. Driving frequency of 196kHz (strip interval of 8mm).

We also studied the effect of more pairs of APS in one column, as in the case of PPM EMAT [6], on the excited SH wave. As seen in Fig.7, the excited LSR decreased slowly with the increasing pairs of APS, it is 16.2% for one pair APS and 13.3% for the four pairs of APS case. As to the half radiation angle of SH wave, it decreases from about 75° (one pair APS) to about 50° (four pairs APS). That is, using more pairs of APS in one column would also suppress the Lamb waves and focus the SH wave energy, but the efficiency is much lower than that of using long strips. Therefore, in practical applications, it is not necessary to use more pairs of APS in one column.

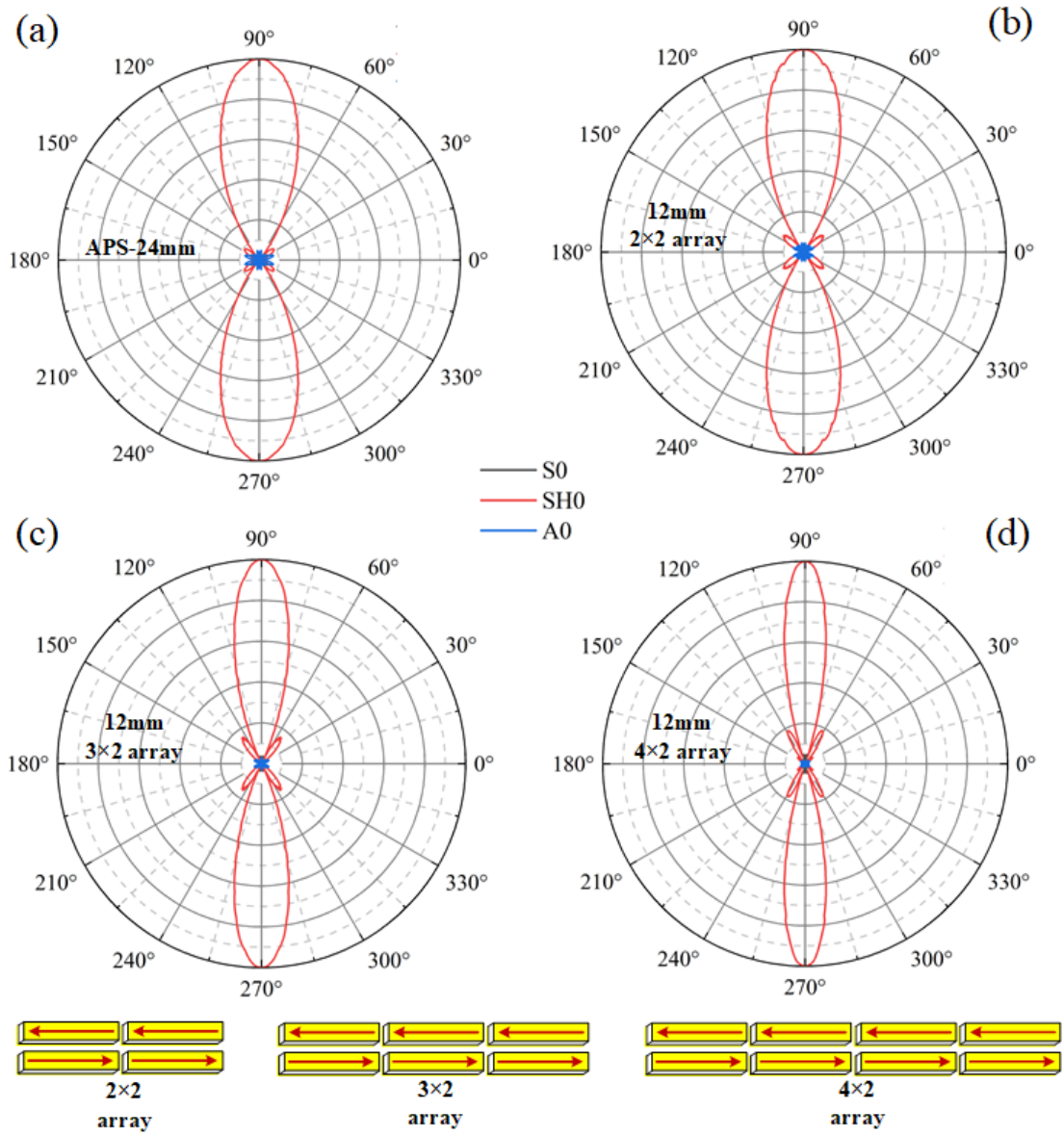


FIG.8 FEM simulated wave patterns excited by using (a) one pair of 24mm-long APS and 12mm-long strips of (b) 2×2 array; (c) 3×2 array; (d) 4×2 array. Driving frequency is 196kHz (strip interval of 8mm).

Although increasing the strip length is very effective in suppressing the Lamb waves and focusing SH wave energy, in practice, long strips are difficult to pole and apt to break in applications. Here we proposed to synthesize a long strip using several short strips, that is, 2×2 array of 12mm-long strips corresponds to a pair of 24mm-long APS,

3×2 array corresponds to 36mm-long APS and 4×2 array corresponds to 48mm-long APS. The simulated wave patterns using these arrays were shown in Fig.8 where the results by 24mm-long APS were also listed. It can be seen that the wave patterns excited by 2×2 array of 12mm-long strips is almost identical to that by the 24mm-long APS, i.e., the Lamb wave were well suppressed. But the grating lobes of SH₀ wave appeared in the 2×2 array case, which is 12.2% of the maximum SH₀ wave amplitude. In the case of the 3×2 array and 4×2 array, the Lamb waves were further suppressed while the grating lobes of SH₀ wave were enhanced to 15.7% and 18.3% of the maximum SH₀ wave amplitude. The grating lobes of SH₀ wave should be caused by the fact that the strip length (or column spacing) of 12mm is larger than the half wavelength (8mm) [41]. If the half wavelength is larger than 12mm, the grating lobes should be well suppressed. This can be verified by the simulation results at 100kHz (half wavelength of 15.5mm), as seen in Fig.9.

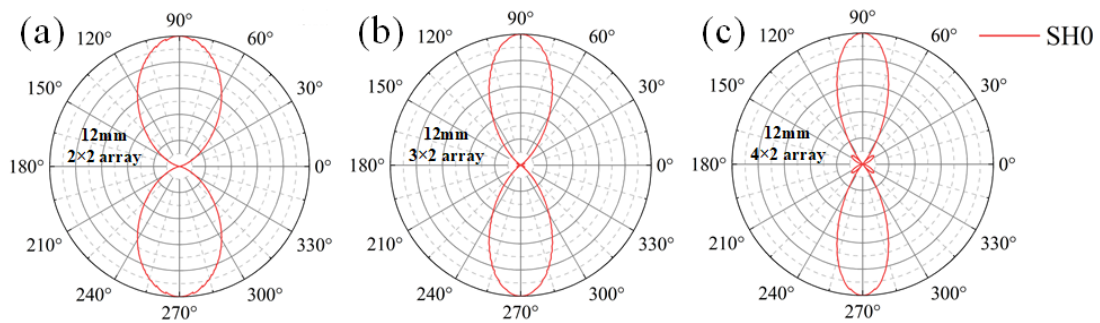


FIG.9 FEM simulated SH₀ wave patterns excited by using 12mm-long strips of (a) 2×2 array; (b) 3×2 array; (c) 4×2 array at 100kHz (strip interval of 15.5mm). Grating lobes of SH₀ were well suppressed.

3.5 Performances of multiple piezoelectric strips in one row

We further simulated the performances of multiple d₁₅ piezoelectric strips in one row in generating guided waves since their performance should be almost equivalent to a very long d₁₅ strip, which can be inferred from Fig.8. The advantage of using multiple strips in one row is that the working frequency can be varied freely in a wide range without reassembling the transducers. Fig.10 shows the FEM simulated guided wave

patterns excited by using four 12mm-long d_{15} PZT strips in one row at 157kHz, 196kHz and 262kHz, respectively. It can be seen that at all frequencies, the Lamb waves were well suppressed with the LSR only about 5%. However, as expected, there appeared grating lobes of SH_0 wave with the amplitude about 20% of the main lobes. Meanwhile, the angle between the SH_0 grating lobes and the main lobes decreases steadily with the increasing frequency, which is about 40° at 157kHz, 32° at 196kHz and 25° at 262kHz.

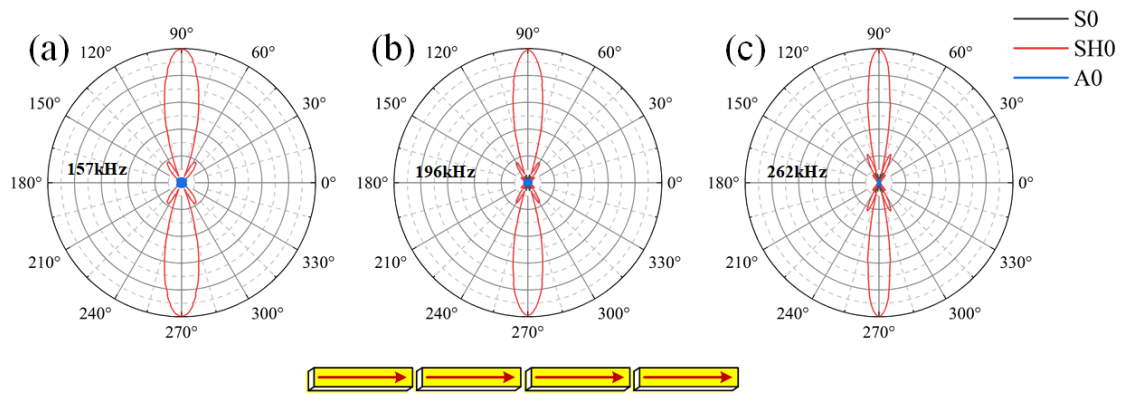


FIG.10 FEM simulated guided wave patterns excited by using four 12mm-long strips in one row at different frequencies: (a) 157kHz; (b) 196kHz; (c) 262kHz.

3.6 Comparison of theoretical and simulated SH_0 wave patterns excited by d_{15} APS

From above simulations results, it can be seen that the radiation angles of the excited SH_0 wave using line forces and d_{15} strips both decrease steadily with the increasing strip length and driving frequency. This tendency is very similar to the single-element bulk longitudinal wave radiation profile in the linear phased array system [42]. Since the SH_0 wave in plates is very similar to that of the bulk longitudinal wave in linear phased array systems, i.e., they are both non-dispersive and two-dimensional, we can anticipate that the theories for the latter may also be valid for the former.

Based on the bulk wave phased array theory [42], the far-field acoustic pressure excited by a single-element transducer with the width of a is expressed by:

$$p(r, \theta, t) = \left(\frac{p_0}{r}\right)^{1/2} \frac{\sin(ka \sin \theta / 2)}{k \sin \theta / 2} \exp\left(-\frac{jka \sin \theta}{2}\right) \exp[j(\omega t - kr)] \quad (2)$$

Where p_0 is the acoustic pressure at the center of the single-element transducer (here the geometry center of the d_{15} APS), k is the wave number, ω is the angular frequency and

$$k = \frac{\omega}{c} = \frac{2\pi}{\lambda} \quad (3)$$

The directivity function of the strip transducer is

$$H_1 = Q \left| \frac{\sin(ka \sin \theta / 2)}{ka \sin \theta / 2} \right| = Q \left| \frac{\sin(\pi a \sin \theta / \lambda)}{\pi a \sin \theta / \lambda} \right| \quad (4)$$

Where Q is a constant or can be treated as unity.

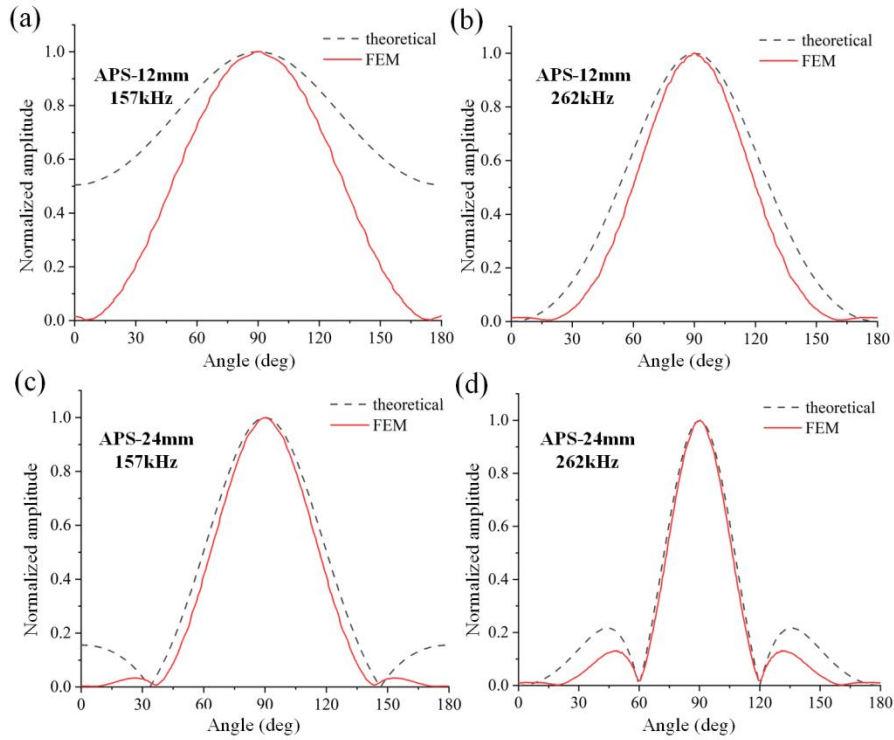


FIG.11 The theoretical and simulated directivity function of SH_0 wave excited by using 12mm-long APS (up) and 24mm-long APS (bottom) under 157kHz ($\lambda=20$ mm) and 262kHz ($\lambda=20$ mm). The ratio a/λ is 0.6, 1.0, 1.2 and 2.0 for (a), (b), (c) and (d), respectively.

Fig.11 shows the theoretical (based on Eq.(4)) and FEM simulated directivity function of the SH_0 wave excited by 12mm-long and 24mm-long APS under 157kHz ($\lambda=20$ mm) and 262kHz ($\lambda=20$ mm), respectively. It can be seen from Fig.11(a) that the theoretical curve cannot fit well with the simulated curve when $a/\lambda=0.6$. This is true because

Eq.(4) can only describe bidirectional radiation profile when $a/\lambda \geq 1.0$ [42]. When this condition is satisfied, as seen in Fig.11(b)-(d), the theoretical curve can fit well with the simulated curve. Furthermore, the larger a/λ , the better fit between the theoretical curves and simulated curves.

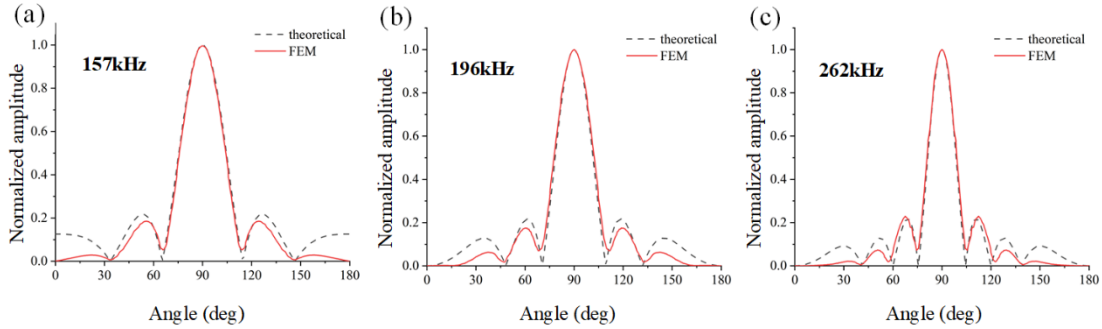


FIG.12 The theoretical and simulated directivity function of SH_0 wave excited by using 12mm-long strips 4×2 array under 157kHz ($\lambda=20$ mm), 196kHz ($\lambda=16$ mm) and 262kHz ($\lambda=20$ mm). The equivalent ratio a/λ is 2.4, 3.0 and 4.0 for (a), (b) and (c), respectively.

As indicated in Section 3.4, several d_{15} strips in one row is almost equivalent to a very long strip in exciting SH wave, we further compare the theoretical and simulated directivity function of SH_0 wave excited by using 12mm-long strips 4×2 array under 157kHz, 196kHz and 262kHz with the equivalent a/λ of 2.4, 3.0 and 4.0, and the results were shown in Fig.12. It can be seen that in all the three cases, the theoretical curves fit almost perfectly with the simulated curves. This further confirmed that Eq.(4) can well predict the radiation profile of the SH_0 wave excited by d_{15} strips when $a/\lambda > 1.0$, and the large a/λ , the better.

4. Experimental results

A series of experimental testing were then conducted to validate the designed bidirectional SH wave transducer. In all the testings, five-cycle sinusoid tone-burst signals with the applied voltage of ??? V were used to drive the bidirectional SH wave transducers.

4.1 Single-frequency property of the APS based bidirectional SH wave transducer

Firstly, the SH wave excitation performances of a single $12 \times 2 \times 0.8\text{mm}^3$ d_{15} piezoelectric strip and antiparallel d_{15} piezoelectric strips (APS) with the interval of 10mm (nominal working frequency of 157kHz) were measured on a 1mm-thick aluminum plate. Another $12 \times 2 \times 0.8\text{mm}^3$ d_{15} strip bonded at 90° direction with the distance of 360mm from the exciter served as the SH wave receiver and the results were shown in Fig.11. It can be seen that for the single d_{15} strip, the amplitude of the excited SH_0 wave appeared at about 75kHz and increased steadily with the frequency up to about 700kHz. In comparison, the responses of the APS also appeared at about 75kHz, it increased quickly with the frequency and reached a peak at about 140.1kHz, which is close to the nominal working frequency of 157kHz. This confirmed that the designed bidirectional SH wave transducer is a single-frequency transducer. The discrepancy between the designed and actual working frequency, which is about 12%, may be due to the finite width (2mm) of the piezoelectric strip or the mounting errors (the two strips may not be perfectly parallel), and such level of discrepancy can be acceptable in practice.

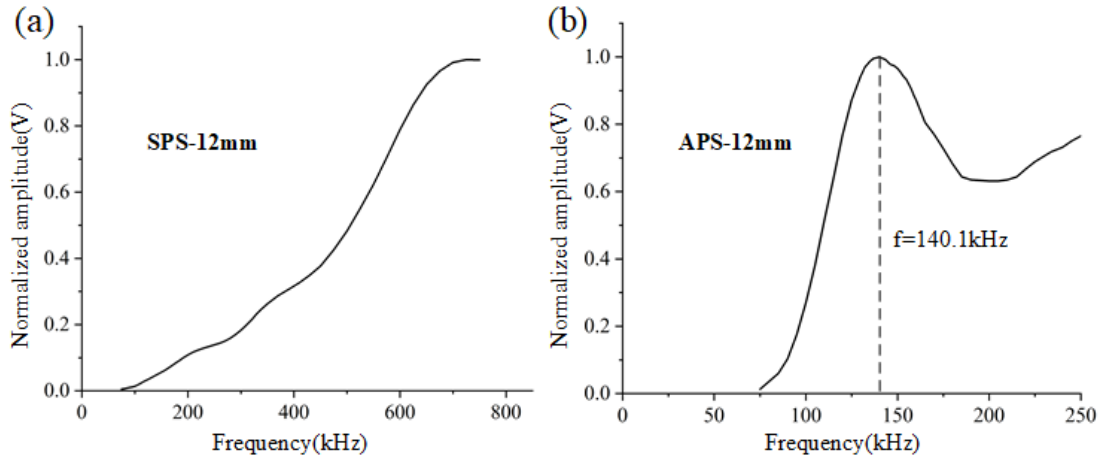


FIG.11 Frequency dependent SH_0 wave excited by (a) a single $12 \times 2 \times 0.8\text{mm}^3$ d_{15} piezoelectric strip and (b) Antiparallel d_{15} piezoelectric strips (APS) with the interval of 10mm (nominal working frequency of 157kHz). Another single d_{15} piezoelectric strip placed at 90° direction serves as the receiver.

4.2 Wave patterns excited by the APS based bidirectional SH wave transducer

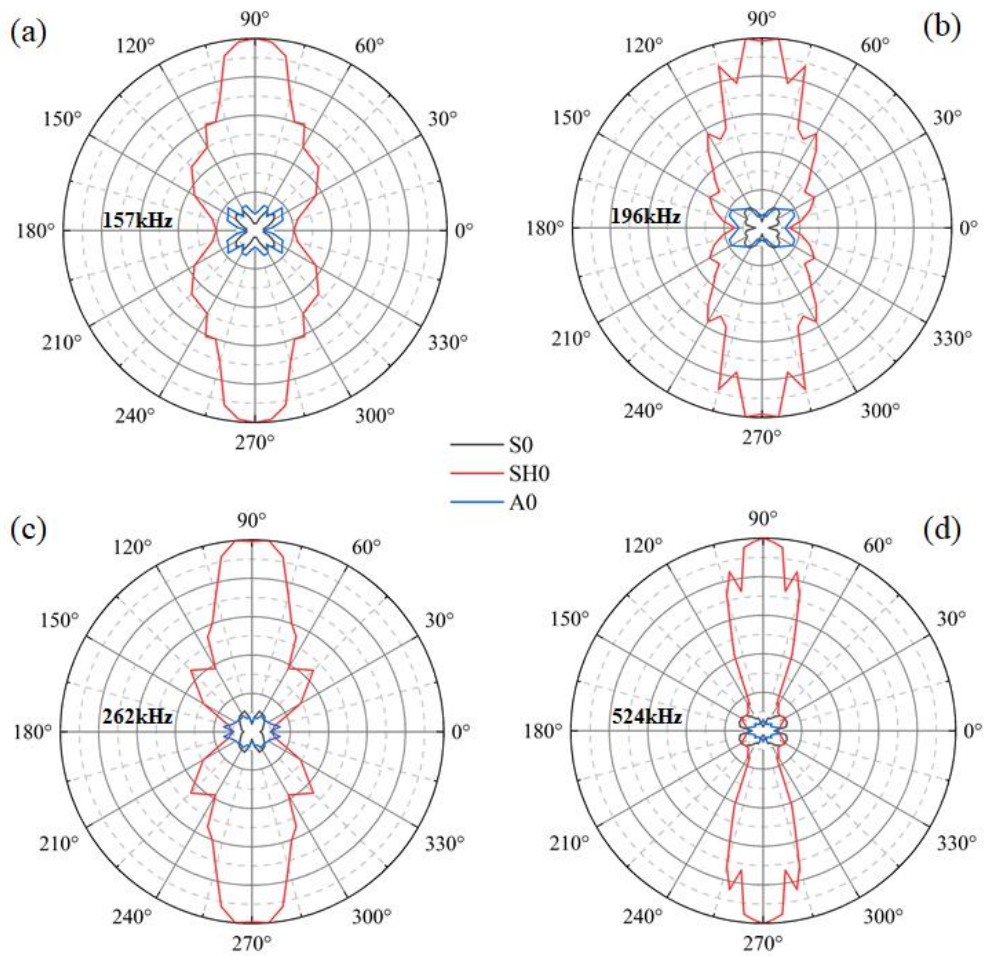


FIG.12 Wave patterns excited by 12mm-long APS with different intervals: (a) 10mm (157kHz); (b) 8 mm(196kHz); (c) 6 mm (262kHz); (d) 3 mm (524kHz).

Then, the wave patterns excited by 12mm-long APS with different intervals (10mm, 8mm, 6mm, 3mm) were measured by using d_{15} PZT strips (for receiving SH waves) and d_{31} PZT disks (for receiving Lamb waves). Since the wave patterns were symmetric about the 0° direction and the 90° direction, measurements were only conducted from 0° to 90° and the results were shown in Fig.12 in which the responses from other directions were obtained by mirroring. It should be noted that because the sensitivity of the d_{15} PZT strip to SH_0 wave, and that of the d_{31} PZT disk to A_0 wave and S_0 wave are different, and the three type sensitivities also vary with frequency, here for each wave mode, the sensitivities were calibrated using the maximum voltage

amplitude and the FEM simulated maximum displacement in Fig.6. For the 3mm interval case (nominal frequency of 524kHz) whose simulation results is lacking, the sensitivities for three wave modes were taken as the same as that for the 6mm case (262kHz).

It can be seen from Fig.12 that consistent with the FEM simulation results in Fig.6, the LSR excited by the APS is within 20% at 157kHz and 196kHz, and is within 15% at 262kHz and 524kHz. Overall, the half radiation angle of the excited SH_0 wave decreases with the increasing frequency, which is also consistent with the simulation results. The non-smooth wave patterns in Fig.12 may be caused by the sensitivity variations between different SH wave and Lamb wave receivers.

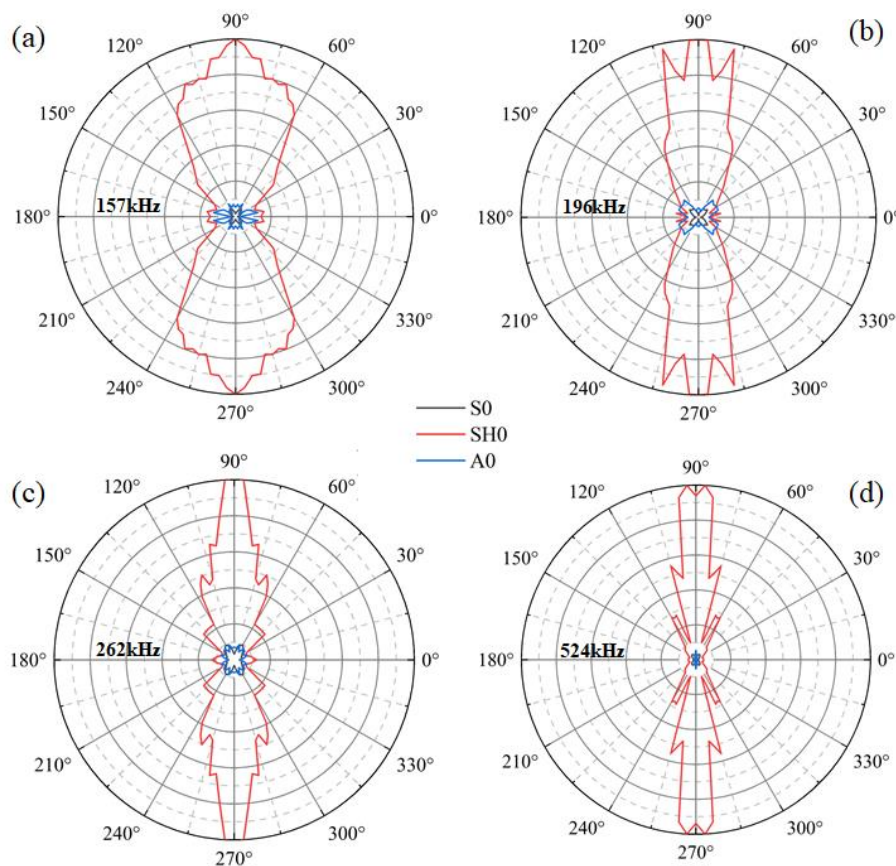


FIG.13 Wave patterns excited by 20mm-long APS with different intervals: (a) 10mm (157kHz); (b) 8 mm(196kHz); (c) 6 mm (262kHz); (d) 3 mm (524kHz).

Fig.13 shows the excited wave patterns by using longer (20mm) APS with different

intervals of 10mm (157kHz), 8mm(196kHz), 6mm (262kHz) and 3mm(524kHz). It can be seen from Fig.13 that consistent with the FEM simulation results in Fig.4, longer APS resulted in smaller LSR, which is about 14% at 157kHz, 12.6% at 196kHz, 10% at 262kHz and 6% at 524kHz. Furthermore, the half radiation angle of excited bidirectional SH_0 wave using longer APS is also smaller than that using shorter ones, which is about 50° at 157kHz, 40° at 196kHz, 30° at 262kHz and 20° at 524kHz. These results confirmed that longer APS is very effective in suppressing the Lamb waves and focusing SH wave. In addition, it can be seen from Fig.13(d) that at 524kHz, there appeared grating lobes of the excited SH_0 wave along the 60° , 120° , 240° and 300° directions, whose amplitude is about 28% of the maximum SH_0 wave amplitude along 90° . Therefore, it should be cautious when using very long strips at high frequency.

4.3 SH_0 wave excited by multiple pairs of APS

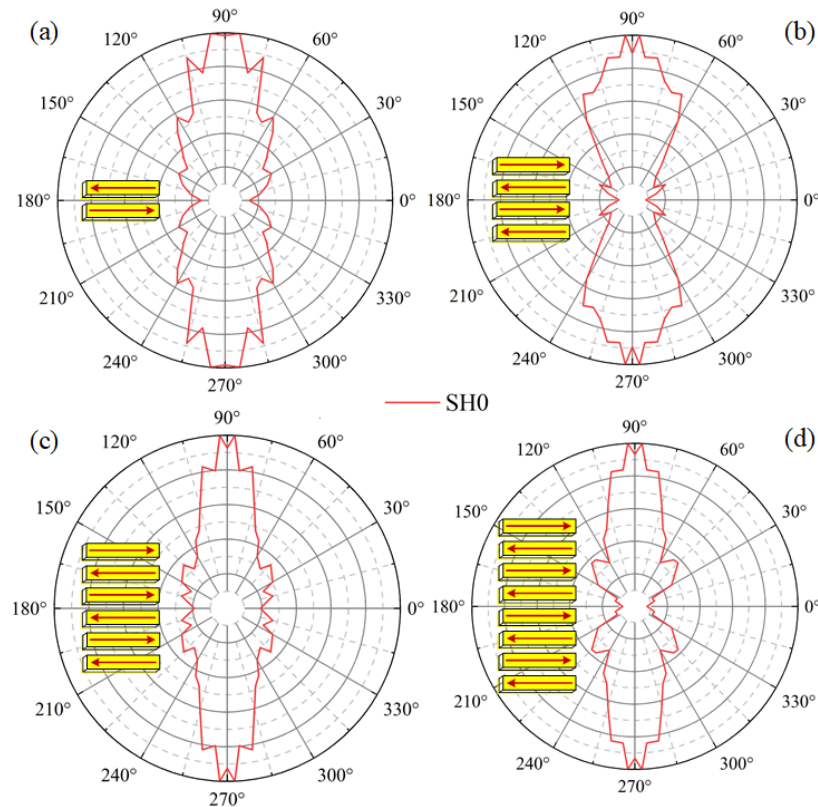


FIG.14 SH_0 waves excited at 196kHz (strip interval of 8mm) by using several pairs of 12mm-long

APS in one column. (a) one pair; (b) two pairs; (c) three pairs. (d) four pairs.

Fig.14 shows the SH_0 waves excited by using several pairs of 12mm-long APS in one column. It can be seen that consistent with the simulation results in Fig.7, increasing the number of APS in one column can reduce the half radiation angle of excited SH_0 wave to some extent, but the efficiency is not high. Therefore, as stated in the simulation results in Section 3.4, it is not necessary to use more pairs of APS in one column.

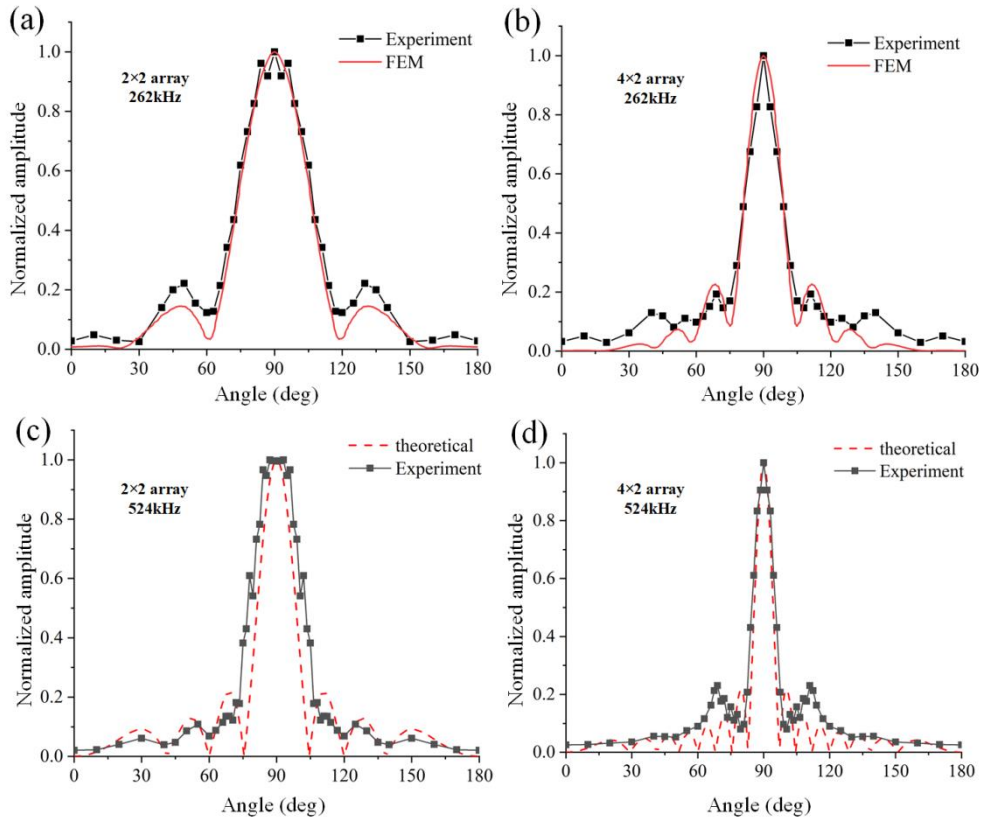


FIG.17 The SH_0 wave radiation patterns excited by using 12mm-long d_{15} strips 2×2 array (left) and 4×2 array (right) at 262kHz (up) and 524kHz (bottom).

Fig.15 shows the excited SH_0 wave patterns by using 12mm-long d_{15} strips 2×2 array and 4×2 array at 262kHz and 524kHz, respectively. It can be seen that consistent with the FEM simulation results in Fig.8, increasing the strip numbers along the row direction is almost equivalent to increasing the strip length, the excited SH_0 wave

energy was greatly focused. The half radiation angle of the SH_0 wave for the 2×2 array case is about 30° at 262kHz and about 20° at 524kHz, while that for the 4×2 array case is only about 15° at 262kHz and about 10° at 524kHz. In Fig.17, the experimental results at 262kHz almost overlap the simulation results, and the experimental results at 524kHz are also consistent with the theoretical curves, especially for the main lobe of the SH_0 wave. This indicated that the bidirectional SH wave radiation patterns excited by several d_{15} strips can be well predicted using FEM simulations or theoretically. Therefore, in practice, to focus the excited SH wave energy, we can use more short d_{15} piezoelectric strips in one row to synthesize very long strips. Meanwhile, increasing the driving frequency would further focus the wave energy and reduce the half radiation angle.

4.4 SH_0 wave excited by multiple d_{15} piezoelectric strips in one row

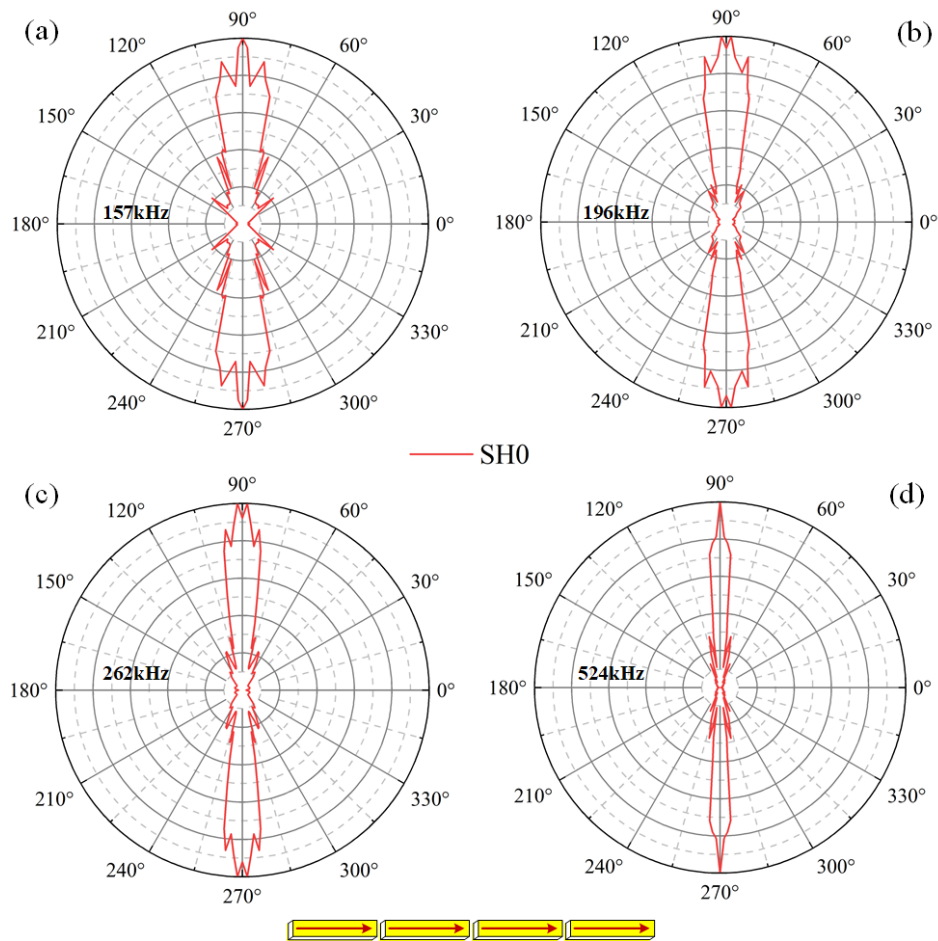


FIG.16 SH₀ waves excited by using four 12mm-long d₁₅ strips in one row at different frequencies:

(a) 157kHz; (b) 196kHz; (c)262kHz; (d)524kHz.

We further examined the performances of four 12mm-long d₁₅ strips in one row in excitation of SH waves at different frequencies and the results were shown in Fig.16. It can be seen that consistent with the FEM simulation results in Fig.10, the multiple strips in one row is almost equivalent to a very long strip, which can effectively focus the SH₀ wave energy. The half radiation angle of SH₀ wave decreases steadily with the increasing frequency, which is also consistent with the 4×2 strip array case in Fig.15. The grating lobes of the excited SH₀ wave are also visible in Fig.16, and their locations is also consistent with the simulation results in Fig.10. At 524kHz where the simulation result is not available, the angle between the grating lobes and main lobes reduced to be only 13°, very close to the half radiation angle of about 10°. That is, at high frequency, the grating lobes can almost be negligible. As mentioned before, the advantage of using multiple strips in one row is that the working frequency can be varied freely.

4.5 Single-mode SH₁ wave excited by APS in a large *fd* plate

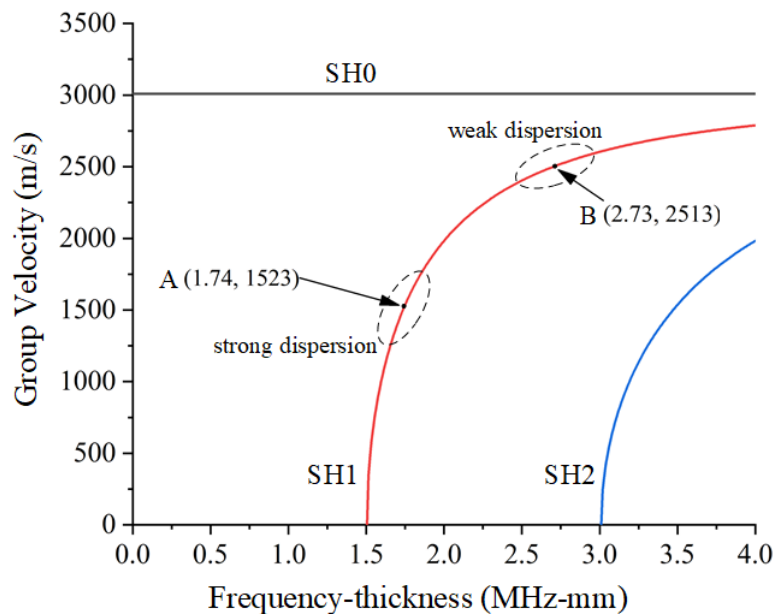


FIG.17 The group velocities versus frequency-thickness product (fd) of first three order SH wave in a large aluminum plate.

As indicated in Section 2.1, in large fd plates, to suppress the SH_0 wave and excite single-mode SH_1 wave, it is required that the strip interval $T = n\lambda_{SH_0} \neq m\lambda_{SH_1}$ (n, m are integers). Here we employed a thick aluminum plate with the dimensions of $1200 \times 400 \times 10 \text{mm}^3$ as the wave guide in which the SH_0 wave velocity is calibrated to be 3010m/s . Firstly, we select the condition of $T = \lambda_{SH_0} = \frac{\lambda_{SH_1}}{2}$ and it is deduced from Eq.(1) that $fd = 1.74 \text{MHz} \cdot \text{mm}$, thus the driving frequency is selected as 174kHz . From the group velocities curves of SH waves in the aluminum plate in Fig.17, it can be seen that here the group velocity of SH_1 wave is 1523m/s (Point A), which is much smaller than that of 3010m/s for the SH_0 wave, thus they can be clearly identified in the time domain when a large travelling distance of 400mm is used.

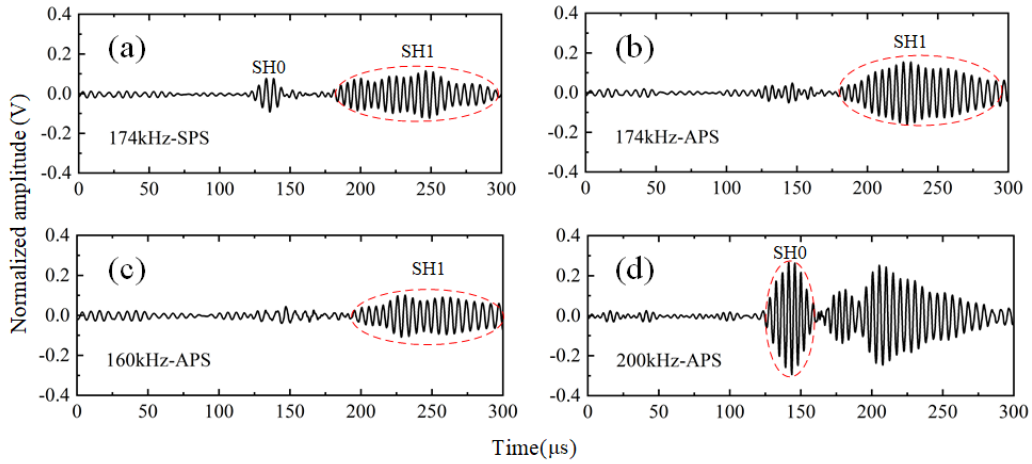


FIG.18 Wave signals excited in a $1200 \times 400 \times 10 \text{mm}^3$ aluminum plate by: (a) four single 12mm -long piezoelectric strips in one row at 174kHz ; (b),(c),(d) 12mm -long APS 4×2 array at 174kHz , 160kHz and 200kHz . Signals received by a 12mm -long d_{15} strip 400mm away from the exciter.

Fig.18(a) shows the SH wave signals excited by using four 12mm -long d_{15} piezoelectric strip in one row at 174kHz , from which it can be seen that both the SH_0 wave and SH_1 wave were clearly separated. Fig.18(b) shows the SH wave signals

excited by 12mm-long APS 4×2 array with the interval of 17.3mm (driving frequency 174kHz), from which it can be seen that the SH_0 wave was well suppressed and the SH_1 wave was strengthened. However, the excited SH_1 wave at 174kHz is strongly dispersive which can be explained by the dispersion curve in Fig.17. At 160kHz, the SH_0 wave were also well suppressed but the SH_1 wave seems not strengthened, seen in Fig.18(c). As expected, at 200kHz, the SH_0 wave were not well suppressed, as seen in Fig.18(d).

We further excited single-mode SH_1 wave with weak dispersion, as denoted by Point B in Fig.17. Here we employed the strip interval of $T = 2\lambda_{SH_0} = 22mm$ and the driving frequency of 273kHz. From Eq.(1), it can be calculated that the group velocity of SH_1 wave at 273kHz is 2513m/s and the wavelength $\lambda_{SH_1} = 9.2mm$, i.e., here $T = 2.4\lambda_{SH_1}$ and the SH_1 wave should also be strengthened to some extent.

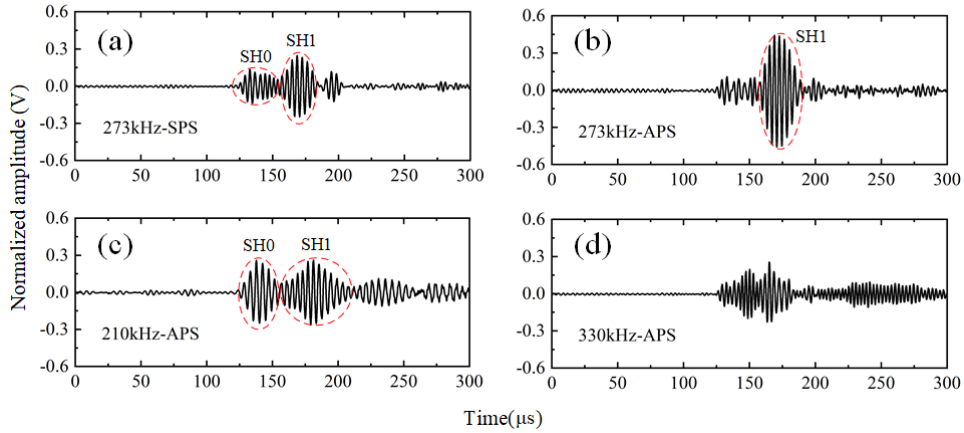


FIG.19 Wave signals excited in a $1200 \times 400 \times 10mm^3$ aluminum plate by: (a) four single 12mm-long piezoelectric strips in one row at 273kHz; (b),(c),(d) 12mm-long APS 4×2 array at 273kHz, 210kHz and 330kHz. Signals received by a 12mm-long d_{15} strip 400mm away from the exciter.

Fig.19(a) shows the SH wave signals excited by using four 12mm-long d_{15} piezoelectric strip in one row at 273kHz, from which it can be seen that the SH_0 wave and SH_1 wave can be just separated. When the APS 4×2 array were used, the excited

SH_0 wave were well suppressed and the SH_1 wave were strengthened, as seen in Fig.19(b). Furthermore, from Fig.19(b), it can also be seen that the SH_1 wave excited at 273kHz were only slightly dispersive, quite different from that excited at 174kHz. As expected, at 210kHz, the SH_0 wave were not suppressed and it can be clearly separated from the SH_1 wave, as shown in Fig.19(c). At higher frequencies, see 330kHz in Fig.19(d), the SH_0 wave and SH_1 wave cannot be clearly separated because their group velocities is very close (3010m/s vs. 2690m/s). Thus, neither can be well suppressed or strengthened.

5 Discussions

From above simulation and experiments results, it can be seen that the d_{15} APS can effectively excited bidirectional SH wave and suppress the Lamb wave. Its working frequency can be conveniently tuned by varying the interval between the strips. Compared with the PPM EMAT based SH wave transducer which requires a ~kW high-power driver [14-16], the APS based transducer proposed in this work can excited SH waves of large amplitude with the drive power less than 1W (applied voltage typically less than 20V). Therefore, the proposed APS based SH wave transducer is expected to replace the EMAT based SH wave transducer when the contact mode is permitted.

The proposed thickness-shear d_{15} APS bidirectional SH wave transducer is also superior to the bidirectional transducer based on dual face-shear d_{24} piezoelectric wafers developed recently [24]. To change the working frequency, the d_{15} APS transducer just needs to vary the strip intervals, while the dual- d_{24} transducer is required to change the dimensions of the d_{24} piezoelectric wafers. Meanwhile, the bandwidth of the d_{15} strip (can reach up to 2MHz when the thickness is below 0.5mm) is considerably larger than that of the square d_{24} wafer (typically below 300kHz). In addition, the large-area electrode configuration of the d_{15} strips is more convenient than the small-area electrode of the d_{24} piezoelectric wafers.

6 Conclusions

In summary, we proposed a bidirectional SH wave transducer based on antiparallel d_{15} piezoelectric strips (APS) whose working frequency can be easily tuned by varying the strip intervals. Both FEM simulations and experimental testing were conducted to validate the proposed bidirectional SH wave transducer. Results show that the excited Lamb waves by single d_{15} piezoelectric strip can well be suppressed by increasing the strip length, reducing the strip interval (increasing drive frequency) or using more numbers of strips. The SH wave radiation angles can be fairly reduced using these measures. Meanwhile, it is found that using several short strips in a row is almost equivalent to a single long strip in excitation of SH waves. The proposed APS bidirectional transducer can also suppress the SH_0 wave and excite single-mode SH_1 wave in a large fd plate.

The proposed APS bidirectional SH wave transducer can be very useful in a variety of fields. i) It can be used to excite bidirectional SH guided waves in plates, Love wave in a thin layer on a semi-infinite space and bulk SH waves in three-dimensional media, which are very essential to study the fundamental properties of SH waves, such as reflection, refraction, mode conversion, etc. ii) It can be used to develop SH wave phase array system, SH wave tomography, etc. for defect locating and sizing in plates [43,44]. iii) It can be used to excite circumferential SH waves for defect inspection in large-diameter pipelines. Due to its good performances, simple structure, tunable design and low cost, the proposed APS bidirectional SH wave transducer is expected to be widely used in above-mentioned areas.

Acknowledgements

This work is supported by the National Natural Science Foundation of China under Grant Nos. 11672003 and 11890684.

References

- [1] F.-K. Chang, Structural health monitoring 2000, CRC Press, 1999.
- [2] D. Alleyne, B. Pavlakovic, M. Lowe, P. Cawley, Rapid, long range inspection of chemical

- plant pipework using guided waves, in: AIP, 2001: pp. 180–187.
- [3] Z. Su, L. Ye, Y. Lu, Guided Lamb waves for identification of damage in composite structures: A review, *J. Sound Vib.* 295 (2006) 753–780.
- [4] V. Giurgiutiu, *Structural health monitoring: with piezoelectric wafer active sensors*, Elsevier, 2007.
- [5] J.L. Rose, *Ultrasonic waves in solid media*, Cambridge university press, 2004.
- [6] C. Vasile, R. Thompson, Excitation of horizontally polarized shear elastic waves by electromagnetic transducers with periodic permanent magnets, *J. Appl. Phys.* 50 (1979) 2583–2588.
- [7] R.B. Thompson, Generation of horizontally polarized shear waves in ferromagnetic materials using magnetostrictively coupled meander-coil electromagnetic transducers, *Appl. Phys. Lett.* 34 (1979) 175–177.
- [8] H. Kwun, C.M. Teller, Magnetostrictive generation and detection of longitudinal, torsional, and flexural waves in a steel rod, *J. Acoust. Soc. Am.* 96 (1994) 1202–1204.
- [9] H. Kwun, I.C.M. Teller, Nondestructive evaluation of non-ferromagnetic materials using magnetostrictively induced acoustic/ultrasonic waves and magnetostrictively detected acoustic emissions, (1995).
- [10] Y.Y. Kim, C.I. Park, S.H. Cho, S.W. Han, Torsional wave experiments with a new magnetostrictive transducer configuration, *J. Acoust. Soc. Am.* 117 (2005) 3459–3468.
- [11] S.H. Cho, S.W. Han, C.I. Park, Y.Y. Kim, Noncontact torsional wave transduction in a rotating shaft using oblique magnetostrictive strips, *J. Appl. Phys.* 100 (2006) 104903.
- [12] H.M. Seung, H.W. Kim, Y.Y. Kim, Development of an omni-directional shear-horizontal wave magnetostrictive patch transducer for plates, *Ultrasonics*. 53 (2013) 1304–1308.
- [13] Y.Y. Kim, Y.E. Kwon, Review of magnetostrictive patch transducers and applications in ultrasonic nondestructive testing of waveguides, *Ultrasonics*. 62 (2015) 3–19.
- [14] R. Ribichini, F. Cegla, P.B. Nagy, P. Cawley, Study and comparison of different EMAT configurations for SH wave inspection, *IEEE Trans. Ultrason. Ferroelectr. Freq. Control*. 58 (2011) 2571–2581.
- [15] N. Nakamura, H. Ogi, M. Hirao, K. Nakahata, Mode conversion behavior of SH guided wave in a tapered plate, *NDT E Int.* 45 (2012) 156–161.
- [16] P. Petcher, S. Dixon, Mode mixing in shear horizontal ultrasonic guided waves, *Nondestruct. Test. Eval.* 32 (2017) 113–132.
- [17] M. Castaings, SH ultrasonic guided waves for the evaluation of interfacial adhesion, *Ultrasonics*. 54 (2014) 1760–1775.
- [18] Z. Wei, S. Huang, S. Wang, W. Zhao, Magnetostriction-based omni-directional guided wave transducer for high-accuracy tomography of steel plate defects, *IEEE Sens. J.* 15 (2015) 6549–6558.
- [19] Z. Liu, X. Zhong, M. Xie, X. Liu, C. He, B. Wu, Damage imaging in composite plate by using double-turn coil omnidirectional shear-horizontal wave magnetostrictive patch transducer array, *Adv. Compos. Mater.* 26 (2017) 67–78.
- [20] P. Wilcox, M. Lowe, P. Cawley, Lamb and SH wave transducer arrays for the inspection of large areas of thick plates, in: AIP, 2000: pp. 1049–1056.
- [21] G. Boivin, M. Viens, P. Belanger, Plane wave SH₀ piezoceramic transduction optimized using geometrical parameters, *Sensors*. 18 (2018) 542.

- [22] H. Miao, Q. Huan, F. Li, Excitation and reception of pure shear horizontal waves by using face-shear d24 mode piezoelectric wafers, *Smart Mater. Struct.* 25 (2016) 11LT01.
- [23] Q. Huan, H. Miao, F. Li, Generation and reception of shear horizontal waves using the synthetic face-shear mode of a thickness-poled piezoelectric wafer, *Ultrasonics*. 86 (2018) 20–27.
- [24] Miao et al. *Ultrasonics* (2018)
- [25] P. Belanger, G. Boivin, Development of a low frequency omnidirectional piezoelectric shear horizontal wave transducer, *Smart Mater. Struct.* 25 (2016) 045024.
- [26] H. Miao, Q. Huan, Q. Wang, F. Li, A new omnidirectional shear horizontal wave transducer using face-shear (d24) piezoelectric ring array, *Ultrasonics*. 74 (2017) 167–173.
- [27] Q. Huan, H. Miao, F. Li, A uniform-sensitivity omnidirectional shear-horizontal (SH) wave transducer based on a thickness poled, thickness-shear (d15) piezoelectric ring, *Smart Mater. Struct.* 26 (2017) 08LT01.
- [28] Q. Huan, M. Chen, F. Li, A practical omni-directional SH wave transducer for structural health monitoring based on two thickness-poled piezoelectric half-rings, *Ultrasonics*. (2018).
- [29] M. Ratssepp, M. Lowe, P. Cawley, A. Klauson, Scattering of the fundamental shear horizontal mode in a plate when incident at a through crack aligned in the propagation direction of the mode, *J. Acoust. Soc. Am.* 124 (2008) 2873–2882.
- [30] P. Rajagopal, M. Lowe, Scattering of the fundamental shear horizontal guided wave by a part-thickness crack in an isotropic plate, *J. Acoust. Soc. Am.* 124 (2008) 2895–2904.
- [31] P. Belanger, High order shear horizontal modes for minimum remnant thickness, *Ultrasonics*. 54 (2014) 1078–1087.
- [32] N. Nazeer, M. Ratssepp, Z. Fan, Damage detection in bent plates using shear horizontal guided waves, *Ultrasonics*. 75 (2017) 155–163.
- [33] X. Yu, M. Ratssepp, Z. Fan, Damage detection in quasi-isotropic composite bends using ultrasonic feature guided waves, *Compos. Sci. Technol.* 141 (2017) 120–129.
- [34] Q. Huan, H. Miao, F. Li, A variable-frequency structural health monitoring system based on omnidirectional shear horizontal wave piezoelectric transducers, *Smart Mater. Struct.* 27 (2018) 025008.
- [35] Q. Huan, M.T. Chen, F.X. Li. A high-resolution structural health monitoring system based on SH wave piezoelectric transducers phased array. (*Ultrasonics* 2019, DOI:)
- [36] P. Li, *MSSP* (2019)
- [37] G. Liu, J. Qu, Guided circumferential waves in a circular annulus, *J. Appl. Mech.* 65 (1998) 424–430.
- [38] X. Zhao, J.L. Rose, Guided circumferential shear horizontal waves in an isotropic hollow cylinder, *J. Acoust. Soc. Am.* 115 (2004) 1912–1916.
- [39] P. Wilcox, M. Lowe, P. Cawley, Omnidirectional guided wave inspection of large metallic plate structures using an EMAT array, *IEEE Trans. Ultrason. Ferroelectr. Freq. Control.* 52 (2005) 653–665.
- [40] Q. Huan, M. Chen, F. Li, A Comparative Study of Three Types Shear Mode Piezoelectric Wafers in Shear Horizontal Wave Generation and Reception, *Sensors*. 18 (2018) 2681.
- [41] B.W. Drinkwater, P.D. Wilcox, Ultrasonic arrays for non-destructive evaluation: A review, *NDT E Int.* 39 (2006) 525–541.
- [42] S.C. Wooh, *Wave Motion* (1999)
- [43] J. Rao, M. Ratssepp, Z. Fan. Limited-view ultrasonic guided wave tomography using an

adaptive regularization method, *Journal of Applied Physics*, 2016, 120(19), 194902.

[44] J. Rao, M. Ratassepp, D. Lisevych, M. Hamzah Caffoor, Z. Fan. On-Line Corrosion Monitoring of Plate Structures Based on Guided Wave Tomography Using Piezoelectric Sensors. *Sensors*, 17 (12), 2882, 2017